



Fast communication

Spectral properties of chaotic signals generated by the skew tent map

M. Eisencraft^{a,b,*}, D.M. Kato^a, L.H.A. Monteiro^{a,b}^a Universidade Presbiteriana Mackenzie, Escola de Engenharia, Pós-graduação em Engenharia Elétrica, Rua da Consolação, n. 896, CEP 01302-907, São Paulo, SP, Brazil^b Universidade de São Paulo, Escola Politécnica, Departamento de Engenharia de Telecomunicações e Controle, Av. Prof. Luciano Gualberto, travessa 3, n. 380, CEP 05508-900, São Paulo, SP, Brazil

ARTICLE INFO

Article history:

Received 2 March 2009

Received in revised form

15 May 2009

Accepted 17 June 2009

Available online 23 June 2009

Keywords:

Chaos

Chaotic communication

Essential bandwidth

Piecewise linear maps

Spectral analysis

ABSTRACT

Chaotic signals have been considered potentially attractive in many signal processing applications ranging from wideband communication systems to cryptography and watermarking. Besides, some devices as nonlinear adaptive filters and phase-locked loops can present chaotic behavior. In this paper, we derive analytical expressions for the autocorrelation sequence, power spectral density and essential bandwidth of chaotic signals generated by the skew tent map. From these results, we suggest possible applications in communication systems.

© 2009 Elsevier B.V. All rights reserved.

1. Introduction

There are a large number of researches involving chaotic signal applications in a variety of areas [1]. When it comes to Signal Processing and Telecommunications, these researches have being intensified after the seminal work by Pecora and Carroll [2]. Since then, the possibilities of applications of chaos in these fields have grown, ranging from digital and analog modulation to cryptography, to generation of pseudorandom sequences, to watermarking, among many others (see e.g. [3–6]). Besides, models of many devices used in signal processing as nonlinear adaptive filters and phase-locked loop networks can present chaotic behavior [7–10].

Here we consider that a limited signal is chaotic if it is deterministic, aperiodic and presents sensitivity to initial conditions [11]. This last property means that, if the

generator system is initialized with a slightly different initial condition, the obtained signal diverges very quickly from the original one. In this paper we focus on one-dimensional discrete-time chaotic signals.

Although there is a large amount of published works on chaos applications in communications, just a few concentrate on spectral characteristics of chaotic signals. Due to the properties that define them, literature uses to consider that they occupy a large frequency range, that they have impulsive autocorrelation sequence (ACS) and that the cross-correlations of signals generated by different initial conditions present low values, see e.g. [3,4,6,12]. Some papers numerically evaluate the power spectral density (PSD) of chaotic signals generated by specific systems, e.g. [13–15]. Sakai and Tokumaru [16] analytically describe the ACS generated by a skew tent family of maps, but do not go further presenting results on the PSD of these signals. Papadopoulos and Wornell [17] deduce the PSD for the tent map and Isabelle and Wornell [18] and Miyaguchi and Aizawa [19] obtained rather general formulas for the PSD of classes of maps. However, to describe the general spectral characteristics of chaotic signals and the consequences they cause when applying these signals in communications is still an open problem.

* Corresponding author at: Universidade de São Paulo, Escola Politécnica, Departamento de Engenharia de Telecomunicações e Controle, Av. Prof. Luciano Gualberto, travessa 3, n. 380, CEP 05508-900, São Paulo, SP, Brazil. Tel.: +55 11 9728 7324.

E-mail addresses: marcioft@mackenzie.br, marcio@lcs.poli.usp.br (M. Eisencraft).

For our studies we have chosen the skew tent map $f_I(\cdot)$ because (i) the signals generated by this map present rich and different behaviors but easily summarized; (ii) it is piecewise linear and their orbits present uniform invariant density which allow analytical calculations; (iii) the tent map studied in [17] is a particular case of the skew tent map permitting comparisons.

Recently, two of us numerically determined the ACS and PSD of the chaotic signals generated by $f_I(\cdot)$ [20]. The objective of this manuscript is to analytically demonstrate these results thus validating them.

The paper is divided into five sections. The map $f_I(\cdot)$ and its main characteristics are described in Section 2. ACS and PSD of the chaotic orbits generated by this map are deduced in Section 3. The relationship between essential bandwidth and Lyapunov exponents is investigated in Section 4. Finally, the conclusions and possible applications of our results are presented in Section 5.

2. Skew tent map

A one-dimensional discrete-time dynamical system or map can be expressed by the difference equation $s(n + 1) = f(s(n))$, where $n \geq 0$ is an integer, $f(\cdot)$ is a function with the same domain and range space $U \subset \mathbb{R}$ and $s(0) \in U$. For each initial condition $s(0) = s_0$, an orbit or signal becomes defined by $s(n, s_0) = f^n(s_0)$ where $f^n(\cdot)$ is the n -th successive application of $f(\cdot)$. For simplicity of notation, an orbit is symbolized by $s(n)$ whenever s_0 is irrelevant.

Here we focus on the skew tent map $f_I(\cdot)$ [21], defined as a modified version of the one proposed in [16]. This piecewise-linear map $f_I(\cdot)$ is given by $s(n + 1) = f_I(s(n))$ where

$$f_I(s) = \begin{cases} \frac{2}{\alpha + 1}s + \frac{1 - \alpha}{\alpha + 1}, & -1 < s < \alpha, \\ \frac{2}{\alpha - 1}s - \frac{\alpha + 1}{\alpha - 1}, & \alpha \leq s < 1, \end{cases} \quad (1)$$

$\{\alpha, s(0)\} \subset U = (-1, 1)$. The parameter α determines the coordinate of the tent peak. Fig. 1(a) illustrates $f_I(\cdot)$ for $\alpha = 0.1$.

It can be shown [22] that the Lyapunov exponent h_I of almost every orbit generated by $f_I(\cdot)$ is a function of α and can be calculated by

$$h_I = \frac{\alpha + 1}{2} \ln\left(\frac{2}{\alpha + 1}\right) + \frac{1 - \alpha}{2} \ln\left(\frac{2}{1 - \alpha}\right) > 0. \quad (2)$$

Thus, the aperiodic signals generated by $f_I(\cdot)$ are chaotic [11]. The maximum value of h_I is $\ln 2$ occurring for $\alpha = 0$.

The invariant density $p(s)$ of the orbits of $f_I(\cdot)$ is uniform [23,24]. In fact, $p(s) = \frac{1}{2}$, $-1 < s < 1$, for any α . This means that samples of the signals generated by this map are uniformly distributed over the interval $(-1, 1)$. So, they are zero-mean and their mean power P is

$$P = \int_{-1}^1 s^2 p(s) ds = \frac{1}{3}. \quad (3)$$

In the following sections, we derive the ACS and PSD of the orbits generated by this map.

3. Autocorrelation sequence and power spectral density

Chaotic signals generated by a map can be considered as sample functions of an ergodic stochastic process [23]. Hence, for a fixed value of α , a sample function can be associated to an initial condition s_0 of $f_I(\cdot)$ generating a chaotic orbit. Bearing this in mind, we can deduce the ACS and the PSD corresponding to $f_I(\cdot)$ as we proceed with ordinary stochastic processes.

3.1. Autocorrelation sequences

The following development employed to deduce the ACS is inspired by [16]. However, in that paper PSD and bandwidth were not analytically calculated.

The ACS $R(k)$ for an integer k is defined by

$$R(k) \equiv E[s(n)s(n + k)], \quad k \geq 0, \quad \forall n \geq 0. \quad (4)$$

The expected value $E[\cdot]$ is taken over all initial conditions that generate chaotic signals. For negative values of k , we conveniently consider

$$R(k) \equiv R(-k), \quad k < 0. \quad (5)$$

In the following deduction, we consider $k \geq 0$ and, to simplify notation, we define $s(n) \equiv x$ and $s(n + k) = f_I^k(x) \equiv y$.

Thus, as y is completely determined by x , the joint probability density function $p(x, y)$ is [25]

$$p(x, y) = p(x)p(y|x) = p(x)\delta(y - f_I^k(x)), \quad (6)$$

where $p(y|x)$ is the conditional density of y given x , $p(x)$ is the invariant density of $f_I(\cdot)$ and $\delta(\cdot)$ is the Dirac unit impulse function [25].

By using $p(s) = \frac{1}{2}$, $-1 < s < 1$ and the sampling property of the unit impulse function [25] then

$$\begin{aligned} R(k) &= E[xy] = \int_{-1}^1 \int_{-1}^1 xyp(x, y) dx dy \\ &= \int_{-1}^1 \int_{-1}^1 xyp(x)\delta(y - f_I^k(x)) dx dy \\ &= \frac{1}{2} \int_{-1}^1 x \left(\int_{-1}^1 y\delta(y - f_I^k(x)) dy \right) dx = \frac{1}{2} \int_{-1}^1 x f_I^k(x) dx. \end{aligned} \quad (7)$$

The map $f_I(\cdot)$ is composed of two linear segments with opposite signal slopes. The image of each of these segments is the domain $U = (-1, 1)$ of the map. Consequently, the graphic of $f_I^k(\cdot)$ is formed by 2^k segments. Fig. 1(a), (b) and (c) are graphics of $f_I(x)$, $f_I^2(x)$ and $f_I^3(x)$ for $\alpha = 0.1$. A fragment of $f_I^k(x)$ for a generic k is shown in Fig. 1(d). The m -th solution of the equation $f_I^k(x) = 1$ is represented by $a_k(m)$, for $1 \leq m \leq 2^{k-1}$. The m -th solution to the equation $f_I^k(x) = -1$ is denoted as $b_k(m)$, where $0 \leq m \leq 2^{k-1}$.

The linear segments from $(b_k(m - 1), -1)$ to $(a_k(m), 1)$ are given by

$$y = \frac{2x - a_k(m) - b_k(m - 1)}{a_k(m) - b_k(m - 1)} \quad (8)$$

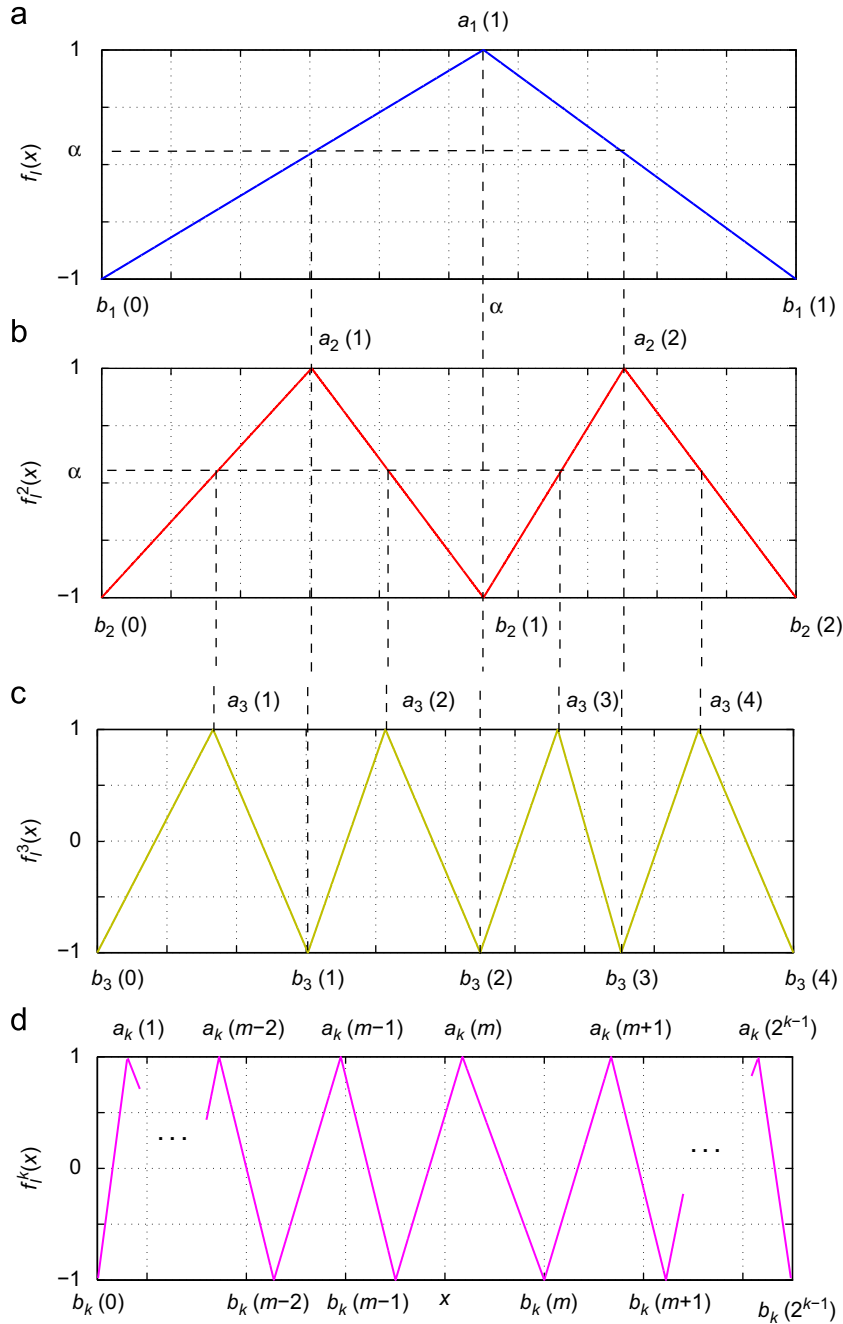


Fig. 1. Maps (a) $f_1(x)$; (b) $f_1^2(x)$; (c) $f_1^3(x)$ for $\alpha = 0.1$. In (d), a fragment of $f_1^k(x)$ for a generic k is shown.

and the linear segments from $(a_k(m), 1)$ to $(b_k(m), -1)$ are given by

$$y = \frac{2x - a_k(m) - b_k(m)}{a_k(m) - b_k(m)}. \tag{9}$$

By substituting Eqs. (8) and (9) in Eq. (7),

$$R(k) = \frac{1}{2} \sum_{m=1}^{2^{k-1}} \left[\int_{b_k(m-1)}^{a_k(m)} x \left(\frac{2x - a_k(m) - b_k(m-1)}{a_k(m) - b_k(m-1)} \right) dx + \int_{a_k(m)}^{b_k(m)} x \left(\frac{2x - a_k(m) - b_k(m)}{a_k(m) - b_k(m)} \right) dx \right]. \tag{10}$$

In order to derive an analytical expression for $R(k)$, both integrals in Eq. (10) must be solved. Thus

$$R(k) = \frac{1}{12} \sum_{m=1}^{2^{k-1}} [(a_k(m) - b_k(m-1))^2 - (a_k(m) - b_k(m))^2]. \tag{11}$$

The process of iterating the map one time, from $f_1^k(x)$ to $f_1^{k+1}(x)$, is illustrated in Fig. 2 where w and z are the roots of $f_1^k(x) = \alpha$. To obtain w and z , y is substituted for α , respectively, on Eqs. (8) and (9) and x is isolated. Thus,

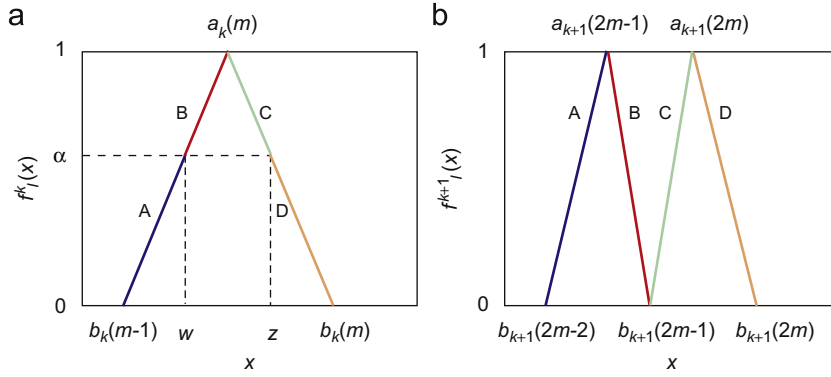


Fig. 2. (a) Fragment of $f_l^k(\cdot)$ and (b) of $f_l^{k+1}(\cdot)$.

these roots are

$$w = \frac{\alpha + 1}{2}(a_k(m) - b_k(m - 1)) + b_k(m - 1), \quad (12)$$

$$z = \frac{\alpha + 1}{2}(a_k(m) - b_k(m)) + b_k(m). \quad (13)$$

Notice that $R(k + 1)$ is given by

$$R(k + 1) = \frac{1}{12} \sum_{m=1}^{2^k} [(a_{k+1}(m) - b_{k+1}(m - 1))^2 - (a_{k+1}(m) - b_{k+1}(m))^2], \quad (14)$$

where from Fig. 2 the following relations are inferred:

$$\begin{aligned} b_{k+1}(2m - 2) &= b_k(m - 1), & a_{k+1}(2m - 1) &= w, \\ b_{k+1}(2m - 1) &= a_k(m), & a_{k+1}(2m) &= z, \\ b_{k+1}(2m) &= b_k(m). \end{aligned} \quad (15)$$

Therefore, $R(k + 1)$ is written as

$$R(k + 1) = \frac{\alpha}{12} \sum_{m=1}^{2^{k-1}} [(a_k(m) - b_k(m - 1))^2 - (a_k(m) - b_k(m))^2]. \quad (16)$$

By comparing Eqs. (11) and (16), then

$$R(k + 1) = \alpha R(k). \quad (17)$$

Solving this difference equation with initial condition $R(0) = P = \frac{1}{3}$ and using Eq. (5), we obtain

$$R(k) = \frac{1}{3} \alpha^{|k|}, \quad (18)$$

for any integer k .

Fig. 3 shows the ACS curves for some values of α .

Observe that $R(k)$ monotonically decays for positive values of α and it oscillates for negative values of α indicating that, in this case, for almost every n and $s(0)$, samples $s(n, s_0)$ and $s(n + 1, s_0)$ have different signals.

In addition, for $\alpha_1 = -\alpha_2$ then

$$R_{\alpha_2}(k) = (-1)^k R_{\alpha_1}(k), \quad (19)$$

where $R_{\alpha_1}(k)$ and $R_{\alpha_2}(k)$ are the ACS for $\alpha = \alpha_1$ and $\alpha = \alpha_2$, respectively.

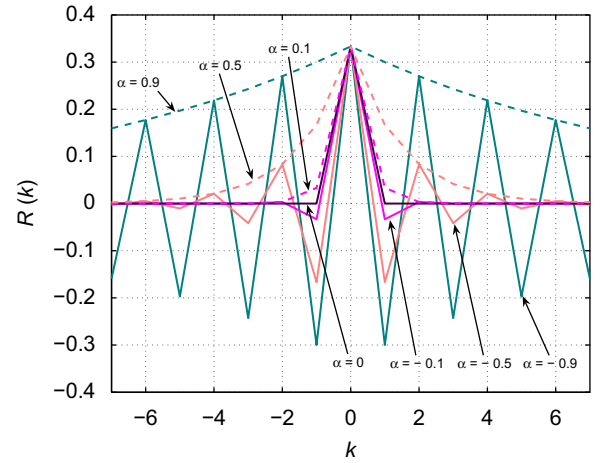


Fig. 3. ACS of signals generated by $f_l(s)$ for different values of α .

These results reveal that chaotic signals do not necessarily have impulsive ACS. This is the case only for $\alpha = 0$, as pointed out by [17].

3.2. Power spectral density

The PSD $S(\omega)$ is the discrete-time Fourier transform (DTFT) of $R(k)$, considering k as the time variable. By calculating the DTFT of Eq. (18), we obtain

$$S(\omega) = \sum_{k=-\infty}^{\infty} R(k) e^{-j\omega k} = \frac{1 - \alpha^2}{3(1 + \alpha^2 - 2\alpha \cos(\omega))}. \quad (20)$$

Fig. 4 shows the PSD for some values of α . The value of α controls the way the power is distributed along the frequency axis. The higher the absolute value of α , the smaller the frequency band where power is concentrated. Furthermore, the signal of α indicates if the concentration occurs in low or high frequency range.

PSDs of signals generated by maps with opposite values of α present symmetry with respect to $\omega = \pi/2$, i.e. if $\alpha_1 = -\alpha_2$, then $S_{\alpha_1}(\omega) = S_{\alpha_2}(\omega + \pi)$, where $S_{\alpha_1}(\omega)$ and $S_{\alpha_2}(\omega)$ are the PSDs of the orbits generated by $\alpha = \alpha_1$ and $\alpha = \alpha_2$, respectively. This frequency shift is a consequence of Eq. (19).

4. Essential bandwidth

PSD properties can be quantified by using the *essential bandwidth* concept. The essential bandwidth B is defined as the length of the frequency interval where $q = 95\%$ of the signal power is concentrated [25]. To calculate B for a signal where the power is concentrated in low frequencies, the equation

$$\int_0^B S(\omega) d\omega = q \int_0^\pi S(\omega) d\omega \quad (21)$$

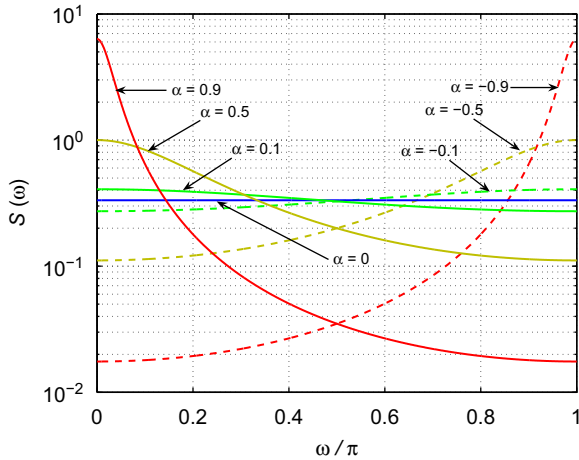


Fig. 4. PSD of the signals generated by $f_I(s)$ for different values of α .

must be solved in B . Because of the symmetry property of $S(\omega)$, the essential bandwidths of signals generated by opposite values of α are equal. Hence, only positive values of α are taken into account here.

By using Parseval's Theorem and Eq. (3), then

$$\int_0^\pi S(\omega) d\omega = \frac{\pi}{3} \quad (22)$$

and the expression for B , written as

$$B = 2 \arctan \left[\tan\left(\frac{q\pi}{2}\right) \left| \frac{\alpha - 1}{\alpha + 1} \right| \right] \quad (23)$$

is obtained by substituting Eqs. (22) and (20) into Eq. (21). Fig. 5 shows as B/π varies with $|\alpha|$ and h_I (given by Eq. (2)). A behavior similar to a white uniform noise process corresponds to the case $\alpha = 0$, because $B/\pi = q = 0.95$ (remember that the invariant density $p(s) = \frac{1}{2}$ is uniform). An extremely narrowband process stands for $\alpha \simeq 1$. Observe that for all values of α , then $h_I > 0$ and the signals are in fact chaotic.

5. Conclusions

In this paper we have analytically deduced the ACS, PSD and essential bandwidth of the chaotic signals generated by the skew tent map. Our exact results are in agreement with the numerical simulations performed by two of us [20].

Our main conclusion is: by adequately choosing the value of α , one can obtain a chaotic signal with the desired bandwidth and with its power concentrated in low or high frequencies.

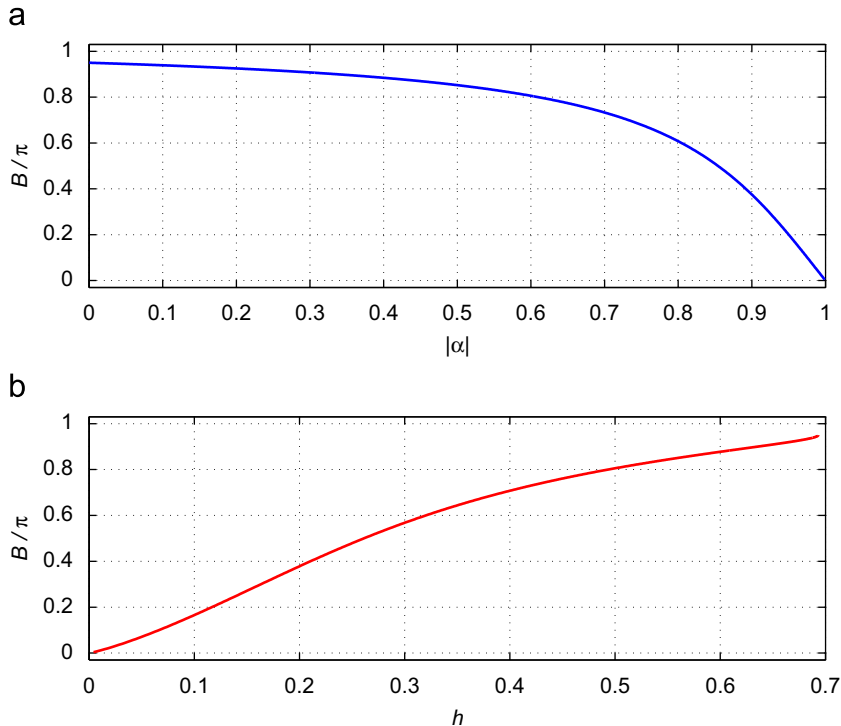


Fig. 5. The value of B/π as function of (a) $|\alpha|$ and (b) Lyapunov exponent h_I .

The analytical expressions presented in this paper confirm the possibility of easily generating chaotic signals with a specific essential bandwidth. This means that the usual assumption about chaos implying broadband uncorrelated signals is not always true.

We have shown how α is related to the essential bandwidth B for the skew tent map. Hence, for a required B , from Eq. (23) the corresponding value of α can be determined and, consequently, the piecewise-linear map that generates chaotic orbits with this particular B .

These results suggest new applications for chaotic signals in communication systems. For instance, different symbols can be associated to different values of $|\alpha|$ and points of orbits generated by the corresponding maps would be transmitted. In the receiver the essential bandwidth of the received signal would be estimated and the value of $|\alpha|$ together with the associated symbol would be determined.

Besides, one can think about frequency multiplexing of chaotic signals as is done in conventional modulations. Using positive and negative values for α it is possible to generate different chaotic signals that can be added and afterwards be separated by using a filter bank [26].

Other possible future direction of work it would be to extend our results to other one-dimensional and even to higher dimensional chaotic signals. We think that it could be possible to model practical signals as speech, images and signals with intermittencies using discrete-time maps that generate chaotic signals with their spectra.

Acknowledgments

D.M. Kato was supported by Mackpesquisa and CAPES. L.H.A. Monteiro is partially supported by CNPq.

References

- [1] S.H. Strogatz, *Nonlinear Dynamics and Chaos: With Applications to Physics, Biology, Chemistry and Engineering*, Perseus Books Group, 2001.
- [2] L. Pecora, T. Carroll, Synchronization in chaotic systems, *Physical Review Letters* 64 (8) (1990) 821–824.
- [3] M.P. Kennedy, G. Setti, R. Rovatti (Eds.), *Chaotic Electronics in Telecommunications*, CRC Press Inc., Boca Raton FL, USA, 2000.
- [4] M. Kennedy, G. Kolumban, Digital communications using chaos, *Signal Processing* 80 (7) (2000) 1307–1320.
- [5] S. Tsekeridou, V. Solachidis, N. Nikolaidis, A. Nikolaidis, A. Tefas, I. Pitas, Statistical analysis of a watermarking system based on Bernoulli chaotic sequences, *Signal Processing* 81 (6) (2001) 1273–1293.
- [6] P. Stavroulakis, *Chaos Applications in Telecommunications*, CRC Press, Inc., Boca Raton, FL, USA, 2005.
- [7] T. Endo, L. Chua, Chaos from phase-locked loops, *IEEE Transactions on Circuits and Systems* 35 (8) (1988) 987–1003.
- [8] B.A. Harb, A.M. Harb, Chaos and bifurcation in a third-order phase locked loop, *Chaos, Solitons & Fractals* 19 (3) (2004) 667–672.
- [9] M.S. Tavazoei, M. Haeri, Chaos in the APFM nonlinear adaptive filter, *Signal Processing* 89 (5) (2009) 697–702.
- [10] L.H.A. Monteiro, A.C. Lisboa, M. Eisenkraft, Route to chaos in a third-order phase-locked loop network, *Signal Processing* 89 (8) (2009) 1678–1682.
- [11] K.T. Alligood, T.D. Sauer, J.A. Yorke, *Chaos: An Introduction to Dynamical Systems*, Springer, New York, 1997.
- [12] I. Djurovic, V. Rubezic, Chaos detection in chaotic systems with large number of components in spectral domain, *Signal Processing* 88 (9) (2008) 2357–2362.
- [13] T. Matsumoto, L.O. Chua, Hyperchaos: laboratory experiment and numerical confirmation, *IEEE Transactions on Circuits and Systems I* 33 (11) (November 1986) 1143–1147.
- [14] K. Ullmann, I.L. Caldas, Transitions in the parameter space of a periodically forced dissipative system, *Chaos, Solitons & Fractals* 7 (11) (1996) 1913–1921.
- [15] G.K. Rohde, J.M. Nichols, F. Bucholtz, Chaotic signal detection and estimation based on attractor sets: applications to secure communications, *Chaos* 18 (1) (2008).
- [16] H. Sakai, H. Tokumaru, Autocorrelations of a certain chaos, *IEEE Transactions on Acoustics, Speech and Signal Processing* 28 (5) (1980) 588–590.
- [17] H.C. Papadopoulos, G.W. Wornell, Maximum-likelihood estimation of a class of chaotic signals, *IEEE Transactions on Information Theory* 41 (1) (1995) 312–317.
- [18] S. Isabelle, G. Wornell, Statistical analysis and spectral estimation techniques for one-dimensional chaotic signals, *IEEE Transactions on Signal Processing* 45 (6) (1997) 1495–1506.
- [19] T. Miyaguchi, Y. Aizawa, Spectral analysis and an area-preserving extension of a piecewise linear intermittent map, *Physical Review E* 75 (6) (2007).
- [20] D.M. Kato, M. Eisenkraft, On the power spectral density of chaotic signals generated by skew tent maps, in: *Proceedings of the International Symposium on Signals, Circuits and Systems 2008*, vol. 1, Iasi, Romania, July 2007, pp. 105–108.
- [21] M. Eisenkraft, L.A. Baccala, The Cramer–Rao bound for initial conditions estimation of chaotic orbits, *Chaos, Solitons & Fractals* 38 (1) (2008) 132–139.
- [22] A. Kisel, H. Dedieu, T. Schimming, Maximum likelihood approaches for noncoherent communications with chaotic carriers, *IEEE Transactions on Circuits and Systems I* 48 (5) (2001) 533–542.
- [23] A. Lasota, M. Mackey, *Probabilistic Properties of Deterministic Systems*, Cambridge University Press, Cambridge, 1985.
- [24] O.A. Rosso, H.A. Larrondo, M.T. Martin, A. Plastino, M.A. Fuentes, Distinguishing noise from chaos, *Physical Review Letters* 99 (15) (2007) 154102.
- [25] B.P. Lathi, *Modern Digital and Analog Communication Systems*, third ed., Oxford University Press, Inc., New York, NY, USA, 1998.
- [26] M. Eisenkraft, D.M. Kato, Spectral properties of chaotic signals with applications in communications, *Nonlinear Analysis: Theory, Methods & Applications*, 2009, in press, doi:10.1016/j.na.2009.05.071.